RÉPUBLIQUE FRANÇAISE
Liberté
Égalité
Fraternité

THE USE OF DEEP LEARNING STRATEGIES FOR SATELLITE INFRARED SPECTROMETER OBSERVATIONS

APPLICATION TO CLOUD PHASE CLASSIFICATION FROM IASI OBSERVATIONS

Eulalie Boucher, Filipe Aires and Marie Doutriaux-Boucher

Scan to download me

LERMA l'Observatoire de Paris | PSL

THALES Building a future we can all trust

cnes

Clouds always cover approximately 60% of the globe [1] and are thus an important part of the climate system. Their detection and classification are vital for the analysis of remote sensing data and validation of climate models [2]. Their identification generally comes from visible and infrared satellite observations that are very sensitive to the presence of clouds and from geostationary satellites, offering continuous measurements.

Most retrieval and classification methods are physics-based [3,4] and performed at the pixel level, but recently Machine Learning (ML) methods have been developed to improve such physical methods [5,6]. Even more recently, **Deep Learning (DL) techniques that seek to exploit spatial structures using image processing have emerged [7], proving that the content in information of neighboring pixels can be useful to detect specific cloud patterns [8].**

In this study, we propose to use **Infrared Atmospheric Sounding Interferometer (IASI) L1c observations** [9] to infer −using an image-processing approach− a **classification of cloud phase into four classes: clear, water, ice, two-level ice**, based on the **SEVIRI-based Optimal Cloud Analysis (OCA)** Climate Data Record (CDR) [10].

DATASETS

IASI L1C Observations [9]

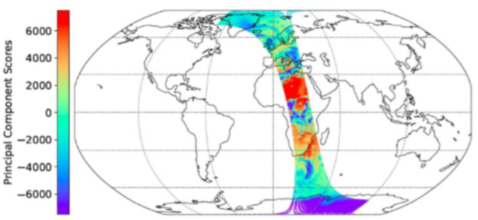

IASI (flying onboard **polar-orbiting** Metop satellites) Principal Component Scores (PCS) of the Band 1 measurements. Original orbit geometry of acquisition is restored to build images of ascending/descending orbits separately.

SEVIRI OCA Cloud Phase [10]

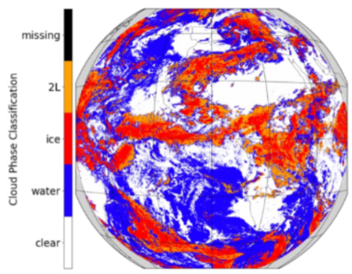

Cloud phase classification (images) coming from SEVIRI, placed onboard the **geo-stationary** satellites Meteosat

Spatio-temporal collocation

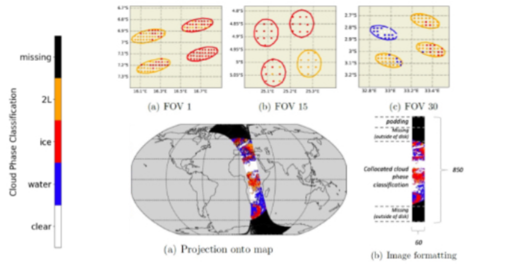

The footprint of each IASI pixel is found by calculating the ellipse equation using the latitude, longitude and satellite azimuth/zenith angles. From there, the cloud phase class assigned to the IASI pixel is **the most common class amongst all SEVIRI points that fall in the ellipse.**

METHODOLOGY

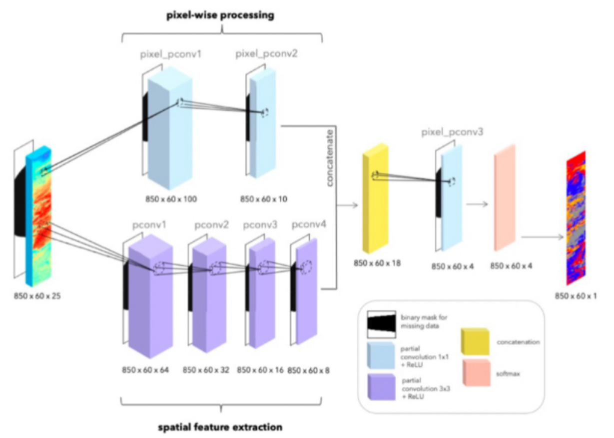

A **Convolutional Neural Network (CNN)** is used. CNNs are one of the most popular image-processing models to exploit the information in neighboring pixels.

During training, all pixels that do not fall over the Meteosat disk are marked as missing (they do not contribute to the loss) because no target output is available. This is made possible using **partial convolutions** [11] that performs the convolution operation only on available pixels. Snow or sea-ice covered pixels are also masked out.

In operational mode, the CNN model is able to infer the cloud phase for **all** pixels of the IASI orbit. A global cloud phase classification is therefore possible.

RESULTS

Results and evaluation over the Meteosat disk

Over the Meteosat disk, direct comparison is performed using the SEVIRI OCA product.

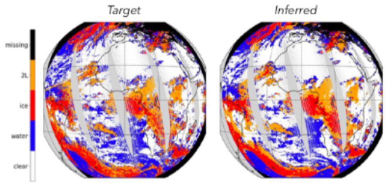

(a) Ascending orbits - 12/02/2019

CNN MODEL — ASCENDING

TARGET CLASSIFICATION \ PREDICTED CLASSIFICATION	clear	water	ice	2L
clear	0.90	0.09	0.0	0.01
water	0.16	0.75	0.03	0.06
ice	0.01	0.16	0.63	0.2
2L	0.03	0.19	0.19	0.59

CNN MODEL — DESCENDING

TARGET CLASSIFICATION \ PREDICTED CLASSIFICATION	clear	water	ice	2L
clear	0.89	0.1	0.0	0.01
water	0.13	0.81	0.04	0.02
ice	0.02	0.21	0.66	0.11
2L	0.01	0.32	0.34	0.33

Results and evaluation outside the Meteosat disk

From the CF proxy, we create a Cloud Fraction product, directly comparable to the AVHRR product

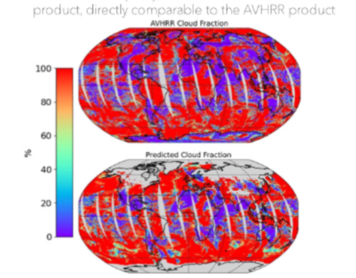

Comparison	Model	Inside Meteosat disk RMS(%)	Inside Meteosat disk STD(%)	Inside Meteosat disk BIAS(%)	Outside Meteosat disk RMS(%)	Outside Meteosat disk STD(%)	Outside Meteosat disk BIAS(%)
CF_{AVHRR}/CF_{SEVIRI}	Ascending	30.5	28.9	-9.8	n/a		
	Descending	32.4	29.9	-12.5	n/a		
CF_{AVHRR}/CF_{CNN}	Ascending	24.6	23.6	-7.0	25.8	24.9	-7.0
	Descending	26.3	24.3	-10.0	28.0	26.0	-10.6

Table 3: Inter-comparison of CF measures (CF_{SEVIRI}, CF_{AVHRR} and CF_{CNN}) inside and outside the Meteosat disk, for ascending and descending models, over the testing set.

Class probabilities as a proxy for the fraction of each class inside each IASI pixel

The CNN is able to downscale to some extent, as the obtained class probabilities output by the network can in fact be compared to the fraction of each class inside each IASI FOV

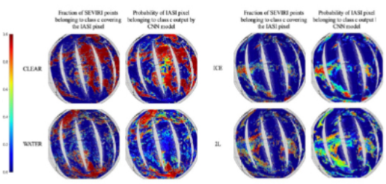

2014-2021 IASI based Cloud Phase Classification Archive

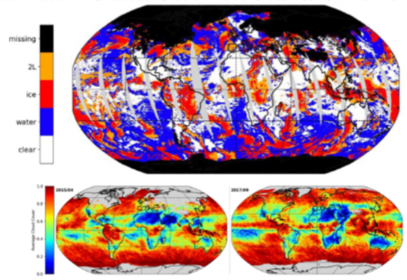

Transforming the IASI orbits into images allows for the use of **CNNs**. Using the neighboring pixels means the neural network can find spatial patterns present in the images which is important for cloud property retrievals. This leads to a good detection and classification of clouds from IASI measurements. With this scheme, ice clouds can be retrieved, which is not possible using a pixelwise approach.

The use of **partial convolutions for training** allows for the use of CNNs on databases with a large amount of missing data and for a near real-time retrieval of full IASI orbits, therefore extending the OCA Cloud Phase Product globally.

The output of the network (i.e., the probability of a pixel being in each class) can in fact be used as a proxy for the fraction of each class inside each IASI pixel. This lets us believe there is a potential to downscale the IASI orbits to SEVIRI spatial resolution.

We reprocessed the entire 2014-2021 Metop-B archive to create a consistent IASI-based Cloud Classification product. The product is available on demand.

[1] Rossow, William B., and Robert A. Schiffer. "Advances in understanding clouds from ISCCP." Bulletin of the American Meteorological Society 80, no. 11 (1999): 2261-2288.

[2] Loeb, Norman G., David A. Rutan, Seiji Kato, and Weijie Wang. "Observing interannual variations in Hadley circulation atmospheric diabatic heating and circulation strength." Journal of climate 27, no. 11 (2014): 4139-4158.

[3] Stubenrauch, C. J., W. B. Rossow, F. Cheruy, A. Chédin, and N. A. Scott. "Clouds as seen by satellite sounders (3I) and imagers (ISCCP). Part I: Evaluation of cloud parameters." Journal of Climate 12, no. 8 (1999): 2189-2213.

[4] Stubenrauch, Claudia J., Artem G. Feofilov, Sofia E. Protopapadaki, and Raymond Armante. "Cloud climatologies from the infrared sounders AIRS and IASI: strengths and applications." Atmospheric Chemistry and Physics 17, no. 22 (2017): 13625-13644.

[5] Aires, Filipe, Francis Marquisseau, Catherine Prigent, and Genevieve Seze. "A land and ocean microwave cloud classification algorithm derived from AMSU-A and-B, trained using MSG-SEVIRI infrared and visible observations." Monthly weather review 139, no. 8 (2011): 2347-2366.

[6] Whitburn, Simon, Lieven Clarisse, Marc Crapeau, Thomas August, Tim Hultberg, Pierre François Coheur, and Cathy Clerbaux. "A CO 2-independent cloud mask from Infrared Atmospheric Sounding Interferometer (IASI) radiances for climate applications." Atmospheric Measurement Techniques15, no. 22 (2022): 6653-6668.

[7] Wang, Xinyue, Hironobu Iwabuchi, and Takaya Yamashita. "Cloud identification and property retrieval from Himawari-8 infrared measurements via a deep neural network." Remote Sensing of Environment 275 (2022): 113026.

[8] Håkansson, Nina, Claudia Adok, Anke Thoss, Ronald Scheirer, and Sara Hörnquist. "Neural network cloud top pressure and height for MODIS." Atmospheric Measurement Techniques 11, no. 5 (2018): 3177-3196.

[9] EUMETSAT (2022): IASI Principal Components Scores Fundamental Data Record Release 1 - Metop-A and -B, European Organisation for the Exploitation of Meteorological Satellites, DOI: 10.15770/EUM_SEC_CLM_0084. http://doi.org/10.15770/EUM_SEC_CLM_0084

[10] EUMETSAT (2022): Optimal Cloud Analysis Climate Data Record Release 1 - MSG - 0 degree, European Organisation for the Exploitation of Meteorological Satellites, DOI: 10.15770/EUM_SEC_CLM_0049. http://doi.org/10.15770/EUM_SEC_CLM_0049

[11] Uhrig, Jonas & Schneider, Nick & Schneider, Lukas & Franke, Uwe & Brox, Thomas & Geiger, Andreas. (2017). Sparsity Invariant CNNs. 11-20. 10.1109/3DV.2017.00012.